Sensors and Materials, Vol. 14, No. 5 (2002) 281–291
MYU Tokyo

S & M 0490

Influence of Initial Layers on Crystallinity of NiO(111) Epitaxial Film Grown at Room Temperature by Pulsed Laser Deposition

Yoshiharu Kakehi, Satoru Nakao, Kazuo Satoh and Tadaoki Kusaka

Technology Research Institute of Osaka Prefecture
Ayumino 2-7-1, Izumi, Osaka 594-1157, Japan

(Received November 21, 2001; accepted June 14, 2002)

Key words: pulsed laser deposition (PLD), room-temperature epitaxy, NiO(111) thin film, sapphire(0001) substrate, higher order epitaxy

Epitaxial thin films of NiO(111) were successfully fabricated on α-Al_2O_3(0001) substrates at room temperature using a pulsed laser deposition method. The oxygen pressure and laser fluence dependences on the film quality, and the relationship between the in-plane lattice parameter and the crystallinity of NiO(111) epitaxial films were investigated. The room-temperature epitaxial growth of NiO(111) thin films on α-Al_2O_3(0001) substrates can be explained by a higher order epitaxy mechanism enabling the fourfold longer in-plane lattice parameters of NiO(111) to match the threefold longer parameters of α-Al_2O_3(0001) with less than a 4.5% misfit. The expansion of the in-plane lattice parameter was caused by the excess oxygen in the epitaxial films, and improve the crystallinity of the films. The reflection high-energy electron diffraction (RHEED) observations for the epitaxial films with good crystallinity showed that the in-plane lattice parameter was extended by about 5% compared with that of the bulk with a film thickness of 1 nm or less. According to the higher order epitaxy mechanism, the improvement of the crystallinity is due to the relaxation of the lattice misfit between the substrate and the film with a film thickness of 1 nm or less.

1. Introduction

Nickel oxide (NiO) is an antiferromagnetic material whose Neel temperature is 523 K. It has a NaCl-type crystalline structure, and is known to become a p-type wide-gap semiconductor when its composition deviates from stoichiometry or when monovalent atoms such as Li^+ are doped. NiO thin films are very useful as the exchange-biased layer of

spin-valve giant magnetoresistance sensors,[1] p-type transparent conducting film for fabricating transparent p-n heterojunctions,[2] and electrochromic devices.[3]

NiO epitaxial films have been used as the epitaxial layers of artificial oxide superlattices with some very interesting structural and magnetic properties.[4,5] In particular, an epitaxial film of NiO(111) has a layered structure in which nickel ions and oxygen ions are alternately stacked and ferromagnetic planes are coupled antiferromagnetically normal to the substrate. Therefore, oxide superlattices consisting of NiO(111) and CoO(111) epitaxial layers have been expected to produce the most direct relationship between modulations in composition and magnetic structure.[6] NiO(111) epitaxial films have generally been prepared on α-Al_2O_3(0001) substrates at a substrate temperature above 100°C. However, the in-plane lattice parameters of NiO(111) are 0.2952 nm for $d_{(110)}$ and 0.1705 nm for $d_{(211)}$, and those of α-Al_2O_3(0001) are 0.4122 nm for $d_{(10\bar{1}0)}$ and 0.2379 nm for $d_{(11\bar{2}0)}$ in the plane. The lattice misfit between $d_{(110)}$ of NiO(111) and $d_{(11\bar{2}0)}$ of α-Al_2O_3(0001) is as large as 24%. It is suspected that this large lattice misfit makes the film surface rougher due to the effect of three-dimensional island growth when the substrate temperature increase and significantly influences both the epitaxial growth and film quality of the deposited film. Accordingly, the substrate temperature should be as low as possible to fabricate NiO(111) epitaxial films with smooth surfaces on α-Al_2O_3(0001) substrates.

Among the various deposition methods available today, pulsed laser deposition (PLD) is advantageous in preparing high-quality thin film at relatively low substrate temperatures, because of the generation of highly excited species through photochemical ablation.[7] It has been reported that oxide thin films on lattice-matched substrates, such as a CeO_2(111) film/Si(111) substrate[8] and a NiO(100) film/MgO(100) substrate,[9] could be grown epitaxially at room temperature by a PLD method. In our previous paper, we reported that NiO(111) thin films could be grown epitaxially on α-Al_2O_3(0001) substrates at room temperature using a PLD method, and that the crystallinity of the epitaxial films was remarkably improved by expanding the in-plane lattice parameter of the film.[10] However, the effect of the expansion of the in-plane lattice parameter on the crystallinity of NiO(111) epitaxial films has not yet been clarified.

In this paper, we describe room-temperature epitaxial growth of NiO(111) thin film on α-Al_2O_3(0001) substrate, oxygen pressure and laser fluence dependences on the film quality of NiO(111) epitaxial films, and the relationship between the in-plane lattice parameter and the crystallinity of NiO(111) epitaxial film. We then discuss the effect of the expansion of the in-plane lattice parameter on the crystallinity of NiO(111) epitaxial films.

2. Materials and Methods

NiO thin films were fabricated using a PLD apparatus with an rf-radical source.[11] A KrF excimer laser beam was focused on the target, which was prepared by sintering NiO powder in air at 1200°C for 72 h. Substrates were α-Al_2O_3(0001) single crystals and were annealed in an oxygen atmosphere at 1000°C before deposition to obtain atomically flat surfaces.[12] NiO thin films were deposited on the substrates at room temperature (30°C) under a repetition frequency of 1 Hz. The distance from the target to the substrate was 40 mm.

The crystalline structure and the crystallinity of deposited films were analyzed with an X-ray diffractometer (XRD) using Cu K_α radiation. The crystallographic orientation was measured by X-ray pole figure using Schulz reflection and reflection high-energy electron diffraction (RHEED) patterns. The surface morphology was investigated by atomic force microscopy (AFM). The film thickness was obtained with a surface profilometer. The electrical resistivity was measured by a conventional four-contact method.

3. Results and Discussion

3.1 *Room-temperature epitaxial growth of NiO(111) thin film on α-Al_2O_3(0001) substrate*

NiO thin films were fabricated on α-Al_2O_3(0001) substrates at various oxygen pressures and laser fluences. Typical XRD and RHEED patterns of NiO(111) epitaxial films are shown in Figs. 1 and 2, respectively. Only NiO(111) and (222) peaks from the film appeared as shown in Fig. 1. Clear streak RHEED patterns were observed and showed sixfold symmetry. The in-plane orientation relationships between the films and the substrates were confirmed to be NiO$[10\bar{1}]$//α-$Al_2O_3$$[10\bar{1}0]$ and NiO$[2\bar{1}\bar{1}]$//α-$Al_2O_3$$[11\bar{2}0]$. Accordingly, NiO(111) thin films were found to be grown epitaxially on α-Al_2O_3(0001) substrates at room temperature using a PLD method.

Unlike the epitaxial growth of a thin film on a lattice-matched substrate, many domains with sizes of about 20 nm were observed on the film surface from AFM images. However, the area rms roughness of the film was as small as 0.30 nm. The pole figure of the {220}

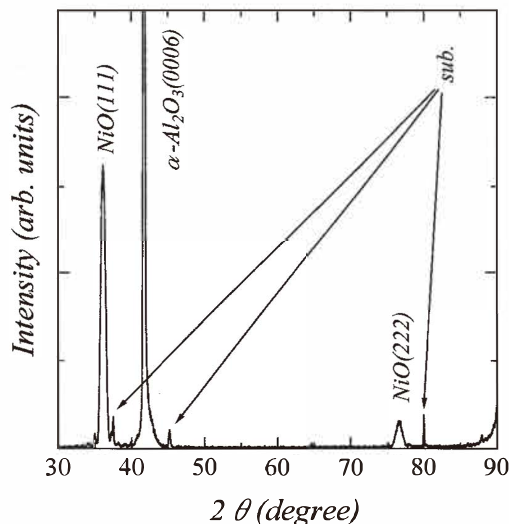

Fig. 1. Typical XRD patterns of NiO(111) epitaxial film. The film was deposited at an oxygen pressure of 1.3 Pa under 3.4 J/cm^2 of laser fluence. Only NiO(111) and (222) peaks from the film appeared.

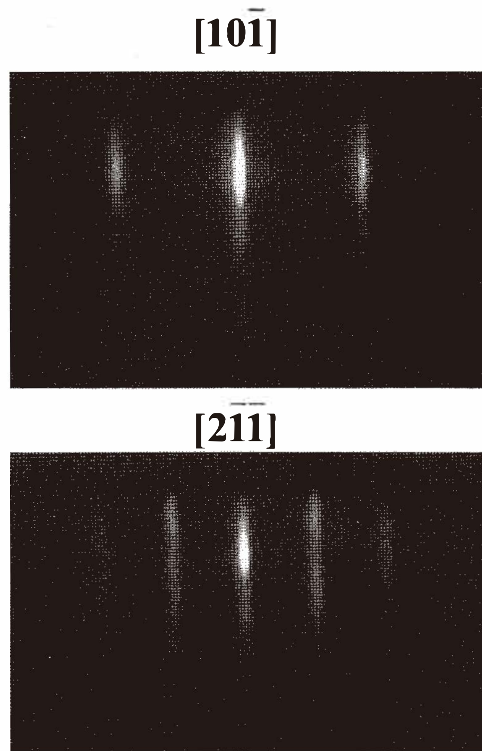

Fig. 2. Typical RHEED patterns of NiO(111) epitaxial film. The film was prepared at the same deposition conditions as that in Fig. 1. The electron beam was incident along the [10$\bar{1}$] and [2$\bar{1}\bar{1}$] azimuths. Clear streak patterns were observed.

planes of the film showed sixfold symmetry and agreed with the RHEED observations. This indicates that each domain can be grown epitaxially on an α-Al_2O_3(0001) substrate at room temperature. Consequently, the room-temperature epitaxial growth of NiO(111) thin films on α-Al_2O_3(0001) substrates can be explained by the higher order epitaxy mechanism.[13] The schematic diagram of the reciprocal lattice for the NiO(111) and α-Al_2O_3(0001) planes is illustrated in Fig. 3. According to this mechanism, the fourfold longer in-plane lattice parameters of NiO(111) match the threefold longer parameters of α-Al_2O_3(0001) with less than a 4.5% misfit. Further details are given elsewhere.[10]

3.2 *Oxygen pressure dependence on film quality of NiO(111) epitaxial film*

The effect of oxygen pressure on the film quality was examined. Figure 4(a) shows the oxygen pressure dependence on both the out-of-plane ($d_{(111)}$) and the in-plane ($d_{(220)}$) lattice parameters of the epitaxial films. NiO(111) epitaxial films were strained compressively due to the large lattice misfit, so $d_{(111)}$ did not depend on the oxygen pressure and was

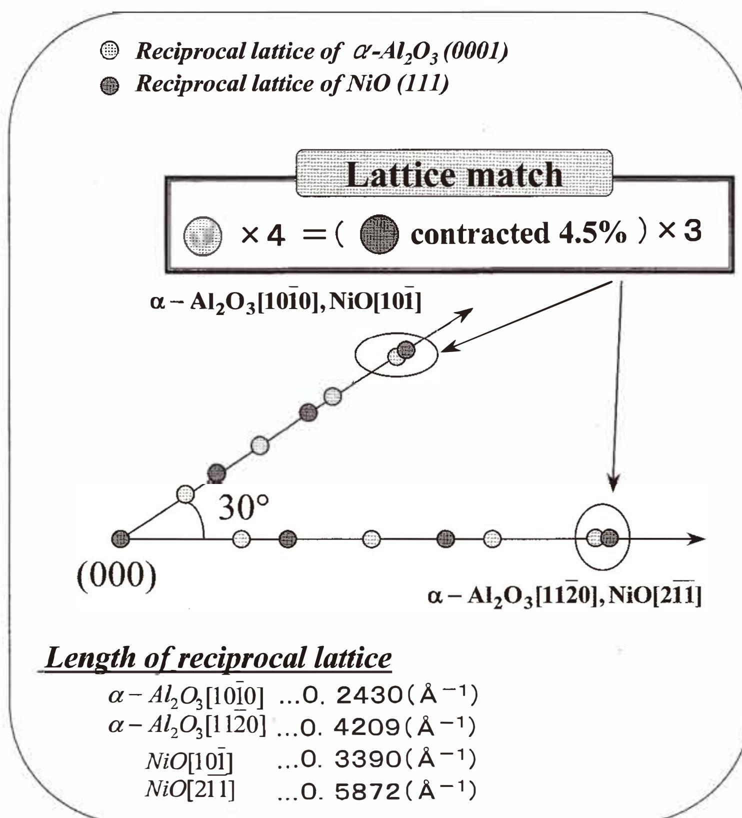

Fig. 3. Schematic diagram of a reciprocal lattice for NiO(111) and α-Al_2O_3(0001) planes based on a higher order epitaxy mechanism. According to this mechanism, the fourfold longer in-plane lattice parameters of NiO(111) match the threefold longer parameters of α-Al_2O_3(0001) with less than a 4.5% misfit.

always larger than that of the bulk. However, $d_{(220)}$ showed a strong dependence on the oxygen pressure and was close to that of the bulk when the oxygen pressure exceeded 1.3×10^{-1} Pa.

The full-width at half maximum (FWHM), which is obtained by rocking curve measurement, and the film thickness of the epitaxial films as a function of the oxygen pressure are shown in Fig. 4(b). The FWHM decreased slightly with increasing oxygen pressure, and then abruptly became small at an oxygen pressure above 1.3×10^{-1} Pa. The film thickness increased with increasing oxygen pressure, and then decreased when the oxygen pressure exceeded 1.3×10^{-1} Pa. These results indicate that the crystallinity of the epitaxial films is significantly improved by expanding $d_{(220)}$ and is independent of the film thickness.

The electrical resistivity measurement of the epitaxial films was carried out at room temperature. The result is shown in Fig. 5. The resistivity increased with increasing

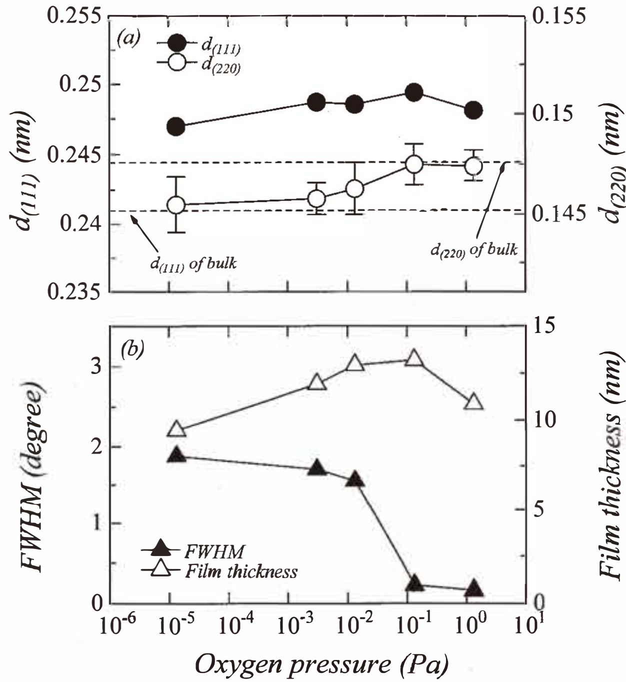

Fig. 4. (a) Dependence on oxygen pressure of both the out-of-plane ($d_{(111)}$) and the in-plane ($d_{(220)}$) lattice parameters of the epitaxial films. (b) FWHM and film thickness of the epitaxial films as a function of oxygen pressure. Laser fluence was 3.4 J/cm^2.

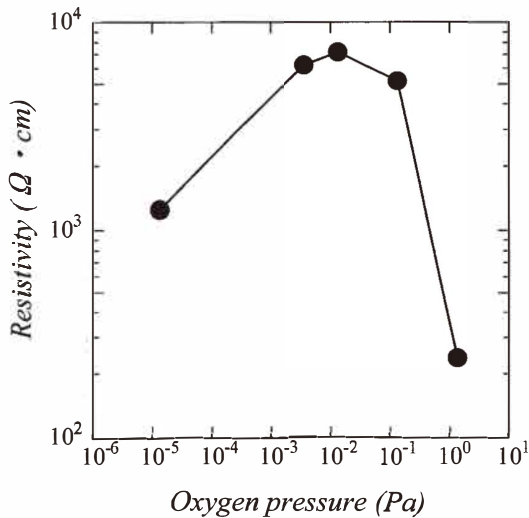

Fig. 5. Oxygen pressure dependence of the electrical resistivity of the epitaxial films. Laser fluence was 3.4 J/cm^2.

oxygen pressure, and then decreased when the oxygen pressure exceeded 1.3×10^{-1} Pa. It is considered that the reduction of the resistivity is caused by the compositional deviation from stoichiometry and the excess oxygen exists in the epitaxial films deposited at an oxygen pressure above 1.3×10^{-1} Pa. Consequently, the existence of the excess oxygen in the epitaxial films was found to be very important for expanding $d_{(220)}$.

3.3 *Laser fluence dependence on film quality of NiO(111) epitaxial film*

The relationships between the film quality and the laser fluence were also investigated when the oxygen pressures were 1.3×10^{-2} Pa and 1.3 Pa. Their results are shown in Figs. 6 and 7, respectively.

When the oxygen pressure was 1.3×10^{-2} Pa, $d_{(111)}$ was always larger than that of the bulk. However, $d_{(220)}$ decreased with increasing laser fluence and became smaller than that of the bulk at a laser fluence above 2.9 J/cm^2. The FWHM increased slightly with increasing laser fluence, and then abruptly became large when the laser fluence exceeded 2.9 J/cm^2. The film thickness increased linearly with increasing laser fluence.

On the other hand, when the oxygen pressure was 1.3 Pa, $d_{(111)}$ was always larger than that of the bulk. However, $d_{(220)}$ increased with increasing laser fluence and was close to that of the bulk at a laser fluence above 2.4 J/cm^2. The FWHM decreased slightly and the

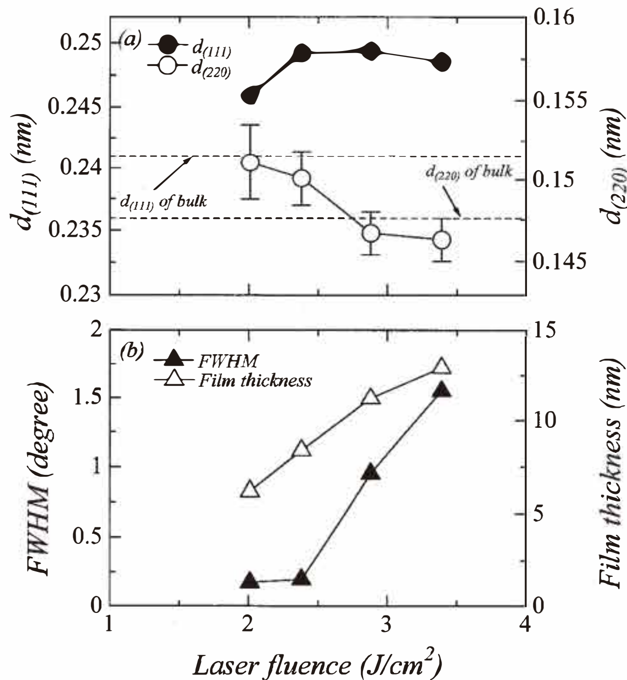

Fig. 6. (a) Dependence on laser fluence of both the out-of-plane ($d_{(111)}$) and the in-plane ($d_{(220)}$) lattice parameters of the epitaxial films. (b) FWHM and film thickness of the epitaxial films as a function of laser fluence. Oxygen pressure was 1.3×10^{-2} Pa.

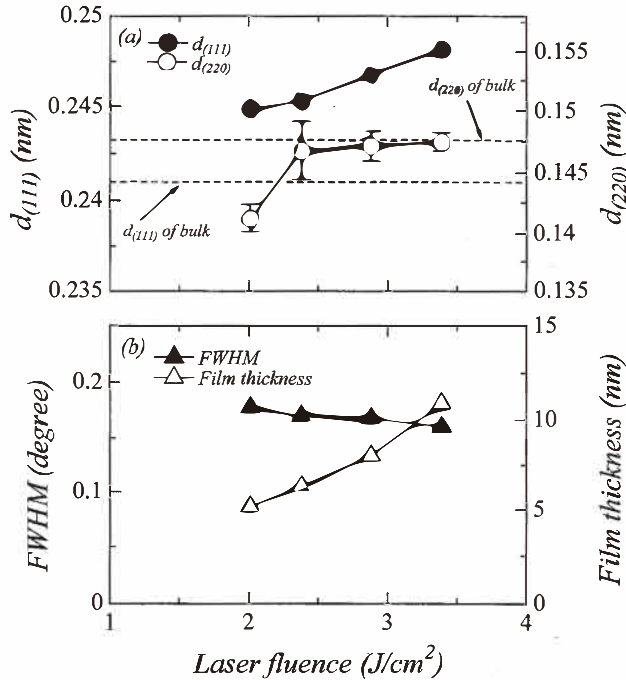

Fig. 7. (a) Dependence on laser fluence of both the out-of-plane ($d_{(111)}$) and the in-plane ($d_{(220)}$) lattice parameters of the epitaxial films. (b) FWHM and film thickness of the epitaxial films as a function of laser fluence. Oxygen pressure was 1.3 Pa.

film thickness increased linearly with increasing laser fluence.

These laser fluence dependences on the film quality suggest that the crystallinity of the epitaxial films is significantly improved by expanding $d_{(220)}$, and that the optimum laser fluence for obtaining the epitaxial films with good crystallinity is largely influenced by the oxygen pressure during deposition. Consequently, the crystallinity of the epitaxial films was found to be improved by extending $d_{(220)}$ to satisfy the deposition conditions that growth species arriving at the substrate could maintain sufficient migration energy for epitaxial growth and that the excess oxygen exists in the epitaxial films at the same time.

3.4 *Relationship between the in-plane lattice parameter and the crystallinity of NiO(111) epitaxial film*

In sections 3.2 and 3.3, the expansion of $d_{(220)}$ was found to be a very important factor in fabricating the NiO(111) epitaxial films with good crystallinity. However, the reason is not clear. Therefore, the RHEED observations were carried out with changing pulse numbers of a KrF excimer laser to investigate the behavior of $d_{(220)}$ during deposition. Figure 8 shows the film thickness dependence on $d_{(220)}$ of the epitaxial films deposited at

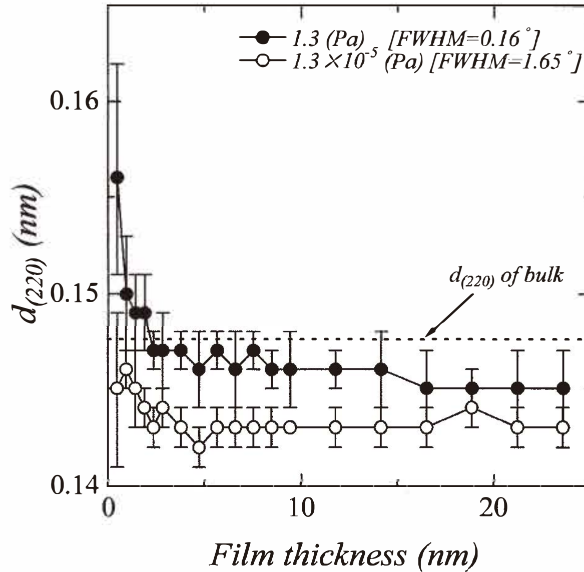

Fig. 8. Film thickness dependence of the in-plane lattice parameter ($d_{(220)}$) of the epitaxial films deposited at different oxygen pressures using the RHEED observations. When the FWHM of the film was as small as 0.16°, the initial layers, in which $d_{(220)}$ was extended by about 5% compared with that of the bulk with a film thickness of 1 nm or less, were observed. However, $d_{(220)}$ did not depend on the film thickness and was always smaller than that of the bulk when the FWHM of the film was 1.65°.

different oxygen pressures. It was found that $d_{(220)}$ was extended by about 5% compared with that of the bulk with a film thickness of 1 nm or less when the FWHM of the film was as small as 0.16°. On the other hand, $d_{(220)}$ did not depend on the film thickness and was always smaller than that of the bulk when the FWHM of the film was 1.65°. Similar results were obtained for the epitaxial films prepared at different laser fluences. This indicates that the crystallinity of the epitaxial films is largely influenced by the initial layers, in which $d_{(220)}$ is extended by about 5% compared with that of the bulk and the film thickness is 1 nm or less. Therefore, a two-step growth method was carried out to confirm the effect of the initial layers on the crystallinity of the NiO(111) epitaxial films. First, the initial layers were prepared on α-Al_2O_3(0001) substrates at an oxygen pressure of 1.3 Pa, and then the films were deposited on them at an oxygen pressure below 1.3×10^{-2} Pa. The FWHM of the epitaxial films with or without the initial layers as a function of the oxygen pressure is shown in Fig. 9. By means of preparing the initial layers, the crystallinity of the epitaxial films showed a remarkable improvement. According to the higher order epitaxy mechanism as shown in Fig. 3, the lattice misfit is found to be close to zero when $d_{(220)}$ is expanded by about 4.5%. Consequently, it was found that the crystallinity of NiO(111) epitaxial films grown on α-Al_2O_3(0001) substrates at room temperature became better due to the relaxation of the lattice misfit between the substrate and the initial layers.

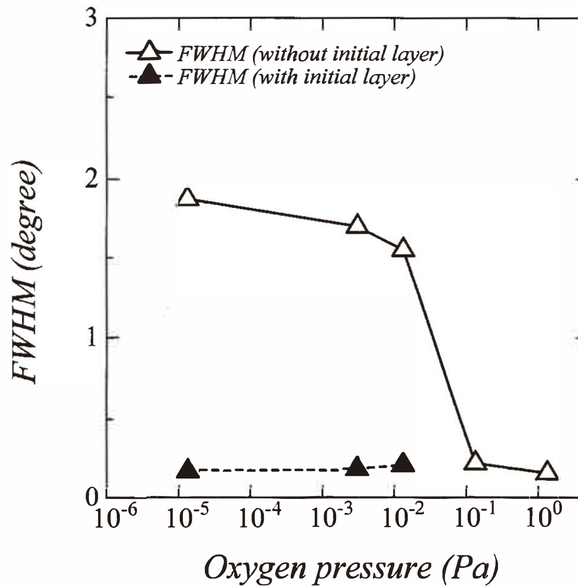

Fig. 9. FWHM of the epitaxial films with and without the initial layers as a function of oxygen pressure. The effect of the initial layers on the crystallinity of the epitaxial films was investigated using a two-step growth method, and a remarkable improvement of the crystallinity was observed. This is due to the relaxation of the lattice misfit between the substrate and the initial layers.

4. Conclusion

NiO(111) epitaxial films were successfully grown on α-Al_2O_3(0001) substrates at room temperature using a PLD method. The oxygen pressure and laser fluence dependences on the film quality, and the relationship between the in-plane lattice parameter and the crystallinity of NiO(111) epitaxial films were investigated. The room-temperature epitaxial growth of NiO(111) thin films on α-Al_2O_3(0001) substrates can be explained by a higher order epitaxy mechanism enabling the fourfold longer in-plane lattice parameters of NiO(111) to match the threefold longer parameters of α-Al_2O_3(0001) with less than a 4.5% misfit. In satisfying the deposition conditions that growth species arriving at the substrate could maintain sufficient migration energy for epitaxial growth and the excess oxygen exist in the deposited films at the same time, the crystallinity of the epitaxial films was improved by expanding $d_{(220)}$. In particular, the RHEED observations and the two-step growth method showed that the initial layers, in which $d_{(220)}$ was extended by about 5% compared with that of the bulk with a film thickness of 1 nm or less, were a very important factor in improving the crystallinity of NiO(111) epitaxial films. According to the higher order epitaxy mechanism, the relaxation of the lattice misfit between the film and the substrate due to the initial layers resulted in improving the crystallinity of NiO(111) epitaxial films grown on a-Al_2O_3(0001) substrates at room temperature.

Acknowledgements

We would like to thank Professor Taichiro Ito, Dr. Norifumi Fujimura and Dr. Atsushi Ashida of Osaka Prefecture University for useful discussions. We also appreciate the kind support of Dr. Hirofumi Chikakiyo of Rigaku Co. who evaluated the NiO(111) film by X-ray pole figure measurement.

References

1 M. J. Carey and A. E. Berkowitz: J. Appl. Phys. **73** (1993) 6892.
2 H. Sato, T. Minami, S. Tanaka and T. Yamada: Thin Solid Films **236** (1993) 27.
3 S. Yamada, T. Yoshioka, M. Miyashita, K. Urabe and M. Kitao: J. Appl. Phys. **63** (1988) 2116.
4 T. Terashima and Y. Bando: J. Appl. Phys. **56** (1984) 3445.
5 G. Chern, D. Berry, D. M. Lind, H. Mathias and L. R. Testardi: Appl. Phys. Lett. **58** (1991) 2512.
6 M. Takano, T. Terashima, Y. Bando and H. Ikeda: Appl. Phys. Lett. **51** (1987) 205.
7 H. Chiba, K. Murakami, O. Eryu, K. Shihoyama, T. Mochizuki and K. Masuda: Jpn. J. Appl. Phys. **30** (1991) L732.
8 M. Yoshimoto, K. Shimozono, T. Maeda, T. Ohnishi, M. Kumagai, T. Chikyo, O. Ishiyama, M. Shinohara and H. Koinuma: Jpn. J. Appl. Phys. **34** (1995) L688.
9 M. Tachiki, T. Hosomi and T. Kobayashi: Jpn. J. Appl. Phys. **39** (2000) 1817.
10 Y. Kakehi, S. Nakao, K. Satoh and T. Kusaka: J. Cryst. Growth. **237–239(P1)** (2002) 591.
11 Y. Kakehi, A. Okamoto, Y. Sakurai, Y. Nishikawa, S. Ogawa and T. Yotsuya: Appl. Surf. Sci. **169–170** (2001) 560.
12 M. Yoshimoto, T. Maeda, T. Ohnishi, H. Koinuma, O. Ishiyama, M. Shinohara, M. Kubo, R. Miura and A. Miyamoto: Appl. Phys. Lett. **67** (1995) 2615.
13 J. Narayan, P. Tiwari, X. Chen, J. Singh, R. Chowdhury and T. Zheleva: Appl. Phys. Lett. **61** (1992) 1290.